Redox Biology 56 (2022) 102457

Contents lists available at ScienceDirect

Redox Biology

journal homepage: www.elsevier.com/locate/redox

Role and mechanism of REG2 depletion in insulin secretion augmented by glutathione peroxidase-1 overproduction

Xi Yan [a,1], Zeping Zhao [a,1], Jeremy Weaver [a], Tao Sun [a], Jun-Won Yun [a,b], Carol A. Roneker [a], Fenghua Hu [c], Nicolai M. Doliba [d], Charles Chipley W. McCormick [a], Marko Z. Vatamaniuk [a,**], Xin Gen Lei [a,*]

[a] Department of Animal Science, Cornell University, Ithaca, NY, 14853, USA
[b] Laboratory of Veterinary Toxicology, College of Veterinary Medicine, Seoul National University, Seoul, 08826, Republic of Korea
[c] Department of Molecular Biology and Genetics, Weill Institute for Cell and Molecular Biology, Cornell University, Ithaca, NY, 14853, USA
[d] Institute of Diabetes, Obesity and Metabolism, University of Pennsylvania, Philadelphia, PA, 19104, USA

ARTICLE INFO

Keywords:
Regenerating islet-derived protein
Glutathione peroxidase
L-type voltage-dependent calcium channel
Glucose-stimulated insulin secretion
Protein-protein interaction

ABSTRACT

We previously reported a depletion of murine regenerating islet-derived protein 2 (REG2) in pancreatic islets of glutathione peroxidase-1 (*Gpx1*) overexpressing (OE) mice. The present study was to explore if and how the REG2 depletion contributed to an augmented glucose stimulated insulin secretion (GSIS) in OE islets. After we verified a consistent depletion (90%, $p < 0.05$) of REG2 mRNA, transcript, and protein in OE islets compared with wild-type (WT) controls, we treated cultured and perifused OE islets (70 islets/sample) with REG2 (1 μg/ml or ml · min) and observed 30–40% ($p < 0.05$) inhibitions of GSIS by REG2. Subsequently, we obtained evidences of co-immunoprecipitation, cell surface ligand binding, and co-immunofluorescence for a ligand-receptor binding between REG2 and transmembrane, L-type voltage-dependent Ca^{2+} channel (CaV1.2) in beta TC3 cells. Mutating the C-type lectin binding domain of REG2 or deglycosylating CaV1.2 removed the inhibition of REG2 on GSIS and(or) the putative binding between the two proteins. Treating cultured OE and perifused WT islets with REG2 (1 μg/ml or ml · min) decreased ($p < 0.05$) Ca^{2+} influx triggered by glucose or KCl. An intraperitoneal (ip) injection of REG2 (2 μg/g) to OE mice (6-month old, $n = 10$) decreased their plasma insulin concentration (46%, $p < 0.05$) and elevated their plasma glucose concentration (25%, $p < 0.05$) over a 60 min period after glucose challenge (ip, 1 g/kg). In conclusion, our study identifies REG2 as a novel regulator of Ca^{2+} influx and insulin secretion, and reveals a new cascade of GPX1/REG2/CaV1.2 to explain how REG2 depletion in OE islets could decrease its binding to CaV1.2, resulting in uninhibited Ca^{2+} influx and augmented GSIS. These findings create new links to bridge redox biology, tissue regeneration, and insulin secretion.

1. Introduction

We previously found that overexpression of selenium-dependent glutathione peroxidase-1 (*Gpx1*) induced type 2 diabetes-like phenotypes in mice [1]. These mice were defined as OE mice and displayed a primary disorder of augmented glucose-stimulated insulin secretion (GSIS) [2,3]. In searching for molecular mechanisms to explain this disorder, we demonstrated a depletion of murine regenerating islet-derived 2 (REG2) in OE islets [4]. Subsequently, we elucidated that the depletion was due to an inhibition of *Reg2* transcription by GPX1-mediated activation of reactive oxygen species (ROS) responsive transcriptional factors (activator protein-1 and albumin D box-binding protein) with binding domains in the proximal promoter of the gene [4]. A remaining key question is if and how the depletion of REG2 contributes to the augmented GSIS in those OE islets.

REG2 represents one of the 12 islet-derived regenerating REG family proteins [5]. The gene (3 kb) contains 6 exons and 5 introns, and the deduced protein peptide contains 173 amino acids (16 kDa) [6]. In the peptide, there are a C-type lectin binding domain [7] and acidic residues potentially involved in $CaCO_3$ crystal binding [8]. Expression of *Reg2* was shown to occur predominantly in pancreatic acinar cells [9–11], but

* Corresponding author.
** Corresponding author.
E-mail addresses: mzv2@cornell.edu (M.Z. Vatamaniuk), XL20@cornell.edu (X.G. Lei).
[1] Co-first authors, equal contribution.

https://doi.org/10.1016/j.redox.2022.102457
Received 10 July 2022; Received in revised form 15 August 2022; Accepted 24 August 2022
Available online 30 August 2022
2213-2317/© 2022 The Authors. Published by Elsevier B.V. This is an open access article under the CC BY-NC-ND license (http://creativecommons.org/licenses/by-nc-nd/4.0/).

Abbreviations

BCIP	5-bromo-4-chloro-3′-indolyphosphate p-toluidine salt
CaV1.2	calcium channel, voltage-dependent, L type, alpha 1C subunit
CM	conditional media
DMF	dimethylformamide
EGFP	enhance green fluorescent protein
EGFR	epidermal growth factor receptor
EXTL3	exostosin like glycosyltransferase 3
FOXA2	Forkhead Box A2
Fura 2-AM/Fluo 4-AM	Fura-2/fluo-4-acetoxymethyl ester
GPX1	glutathione peroxidase 1
GSIS	glucose stimulated insulin secretion
HEK293T	human embryonic kidney 293 cells
hReg1β	human regenerating islet derived protein 1 Beta
INGAP	islet neogenesis associated protein
INS-1	rat insulinoma cell line
Ins1	insulin
NBT	nitro-blue tetrazolium chloride
OE	overexpression
PDX1	pancreatic and duodenal homeobox 1
PNPP	*para*-nitrophenylphosphate
REG1	2, and 3, regenerating islet derived proteins 1, 2, and 3
REG1A	regenerating islet derived protein 1 alpha
REG2 M1 and M2	REG2 mutant 1 and 2
REG3A	regenerating islet derived protein 3 alpha
ROS	reactive oxygen species
WT	wild-type

not in endocrine pancreas under normal conditions [9,12]. However, several groups actually detected mRNA and(or) protein of REG2 in islets of wild-type (WT) mice [4,13–15]. Likewise, expression of the putative human orthologue hREG1β was detected in human pancreas and pancreatic cell lines [16], but not consistently in beta cells [17,18]. Nevertheless, *Reg2* expression was activated or up-regulated in islet regeneration induced by partial pancreatectomy [19], pancreatitis [9], type 1 diabetes [14], and type 2 diabetes and obesity [20]. Similar to other REG proteins including REG1 and INGAP, REG2 is considered to act as a trophic factor in promoting pancreatic beta cell proliferation and regeneration [5]. However, this function was not proved experimentally by the knockout of *Reg2* in mice [12].

With a canonical C-type lectin binding domain [7], REG2 could potentially bind glycoproteins on cell surface that may be involved in GSIS [21,22]. Indeed, L-type voltage-dependent Ca^{2+} channel (VDCC) CaV1.2 is a transmembrane protein and possesses a dihydropyridine structure [23] that specifically binds to immobilized lectins [24]. Thus, CaV1.2 plays a major role in regulating the glucose-stimulated elevation of Ca^{2+} influx upon membrane depolarization to induce insulin exocytosis in the K_{ATP}-dependent pathway [25]. Deletion of *CaV1.2* in mice [26], knockdown of the gene in INS-1 cells [27], and altering CaV1.2 function [28] were shown to affect or impair GSIS. Meanwhile, REG2 was reported to potentially function as an auto-, para-, or endocrine molecule [9]. The protein was produced and secreted into the media by cultured islets [4] and was co-localized with insulin in islet beta cells [14]. Therefore, we hypothesized that REG2, via its C-type lectin binding domain, could bind carbohydrate moiety of the transmembrane CaV1.2 in a ligand-receptor fashion to inhibit glucose-induced Ca^{2+}influx and insulin secretion in pancreatic islets, whereas depletion of REG2 in OE islets result in a loss of this inhibition and contribute to the augmented GSIS.

2. Methods

2.1. Animals, gene expression, and immunoblotting

Our protocol was approved by the Institutional Animal Care and Use Committee of Cornell University. The genetic background of OE and WT mice (C57B1 × C3H), feeding, and pancreas harvesting were the same as previously described [3,4]. Mice were housed in shoeboxes (3–5/box) placed in the East Campus Core Facility of Cornell University (Ithaca, NY), had free access to food and water under a 12h:12h light and dark cycle, and checked daily. All mice used in this research were 2 month-old males unless otherwise indicated.

Because our previous research demonstrated that GSIS differences between WT and OE islets resembled those between the two genotypes of mice [2], we chose islets as the primary experimental model for determining roles and mechanisms of REG2 in the present study. Islets were isolated from WT and OE mice and recovered in RPMI 1640 media (Gibco, Grand Island, NY) (10% fetal bovine serum (FBS), 2 mmol glutamine/l, 10 mmol glucose/l, and 1% PenStrep for 12 h [3,4]. To verify a specific depletion of REG2 in OE islets, relative mRNA abundances of *Reg1* and *Reg2*, along with those involved in insulin synthesis and secretion were quantified (Q-PCR) using total RNA extracted from islets (70 per sample) of WT and OE mice (n = 6) [2]. The primers are listed in Supplemental Table 1. Genotype differences in pancreatic islet (70 per sample) *Reg2* mRNA levels were determined at ages of 6 weeks, 6 months, and 12 months (male, n = 6). To determine *Reg1* and *Reg 2* transcript numbers in pancreatic islets (70 per sample) of WT and OE mice (6-month old, male, n = 6), we amplified the two gene fragments and inserted them into the pPICZ vector (Supplemental Table 3). A serial dilution of the pPICZ constructs, ranging from 1 to 1×10^7 copies/μl was used to establish standard curves for both genes. Concentrations of the plasmids were measured using a fluorimeter. CT values of both genes in testing islets and standard plasmids were obtained by Q-PCR, and the corresponding transcript numbers were calculated based on the CT values against the standard curves. Immunoblotting of REG2 protein (75 μg protein per sample) in pancreatic islets of WT and OE mice (6-month old, male, n = 4) was performed using primary and secondary antibodies listed in Supplemental Table 2 [4].

2.2. Preparation of recombinant REG2 protein and mutants

To determine effects of REG2 on GSIS and the protein structure required for the action (see below), we prepared three constructs including the native form of REG2 and two mutants (REG2 M1 & M2) and overexpressed them in *Pichia pastoris* yeast. REG2 M1 was designed to mutate the C-type lectin binding domain [7] by substituting three amino acid residues in the domain with alanine (G142A, K157A, and D158A) (Fig. 2B and Supplemental Fig. 2). REG2 M2 was designed to substitute the acidic residues potentially involved in $CaCO_3$ crystal binding [8] with glycine (E59G, D60G, E66G, D158G, E159G, and E162G) (Fig. 2B and Supplemental Fig. 3). The NOD mouse *Reg2*cDNA (NM 009043, G22 to A173) [13] was inserted into a *P. pastoris* expression vector *pPICZ* (Invitrogen, Grand Island, NY) in a way that allowed expression of REG2 without non-native amino acids at the N-terminus. The REG2 mutants were created by site-directed mutagenesis of the *Reg2/pPICZgamma C* construct through touchdown PCR using mutagenic forward and reverse primers (Integrated DNA Technologies, Coralville, IA) with PrimeSTAR HS DNA polymerase (Takara, Otsu, Shiga, Japan) followed by Dpn1 digestion of parental DNA template (Supplemental Table 3). The isolated *Reg2* plasmids were transformed into *P. pastoris* GS200 using electroporation (BTX, Holliston, MA), and cultured in BMMY media for 5 d. The secreted REG2 and mutant

proteins were isolated, purified by ammonium sulfate precipitation and ion-exchange chromatography, and verified by SDS-PAGE and immunoblotting [29].

2.3. Effects of REG2 and(or) mutants on GSIS in OE islets and mice

To determine if augmented GSIS in OE islets could be rescued by administrations of REG2, we treated OE islets with the native form of REG2 and(or) the two mutants in static culture and(or) perifusion system. In the static culture, islets were isolated from OE mice (n = 4) and recovered in the RPMI 1640 media as described above for 5 h at 37 °C, 95% air, and 5% CO_2. Thereafter, the islets (70 per sample) were transferred to Krebs buffer containing glucose at 2.8 mmol/l with or without REG2 (1 μg/ml) (3 treatment groups) and incubated in a 37 °C water bath for 0.5 h. The REG2 dose was chosen from a preliminary experiment (0–10 μg/ml) and was in range of reported plasma concentrations of human and mouse REG3 proteins [30]. Subsequently, two groups of islets were treated with 30 mmol glucose/l with or without REG2 (1 μg/ml) for 1 h. The other group of islets was kept the same glucose concentration (2.8 mmol/l) without REG2 as control over the period of time. Supernatants were collected at the ends of the first 0.5 h and the later 1 h treatment for insulin analysis using an ELISA kit [3].

In the perifusion system [31], freshly isolated islets (70 per sample) from OE mice (n = 4 per treatment by genotype) were pre-conditioned with Krebs buffer (pH 7.4, 10 mmol glucose/l) for 1 h and placed on a nylon filter in a plastic perifusion chamber (Millipore, Bedford, MA). The perifusion apparatus consisted of a water bath (37 °C), a fraction collector, and a fast protein liquid chromatography (Bio-Rad, Hercules, CA). The perifusate was a Krebs bicarbonate buffer (pH 7.4) containing Ca^{2+} (2.2 mmol/L) and 0.25% bovine serum albumin equilibrated with 95% O_2/5% CO_2, and the flow and collection rates were 1 ml/min. Effects of REG2 and REG2 M1 and M2 on GSIS were determined by perifusing OE islets with these proteins (at 1 μg/mL/min) or the Krebs buffer for 15 min, followed by a glucose ramp of 0–50 mmol/l (1 mmol/min) [31]. The maximal islet secretion response was tested at the end of each experiment with 30 mM KCl/l after a washout of glucose. Fractions were collected at 1 ml/min for insulin analysis.

To determine *in vivo* effects of REG2 on GSIS in OE mice (6 months old, male, n = 10), we gave them each an intraperitoneal (ip) injection of filter-sterilized REG2 protein (2 μg/g body weight) or an equal volume (10 μL/g) of phosphate-buffed saline (PBS) at 15 min before an ip injection of glucose (1 g/kg). The injected REG2 dose was chosen from a preliminary experiment (0–4 μg/g) and was similar to the dose of REG3δ injected to dogs [32]. Plasma samples were collected at −15, 0, 15, 30, and 60 min after the glucose injection for insulin [3].

2.4. Co-immunoprecipitation of CaV1.2 with REG2 protein and antibody

To determine if REG2 could pull down CaV1.2, we inserted the *CaV1.2* gene into *pcDNA3.0* vector (Addgene, Supplemental Table 3) to generate *pcDNA-CaV1.2* plasmid, and transfected it (4 μg DNA) into beta-TC3 cells (ATCC, Manassas, Virginia, seeded in 6-well plates at 3 × 10^5/well and 80% confluency at transfection) using lipofectamine™2000 (Invitrogen). The cells were cultured in DMEM (Gibco) containing 15% FBS, 1% PenStrep, 1% sodium pyruvate, HEPES (25 mmol/l), 0.4% fungizone, and 0.0004% beta-mercaptoethanol at 5% CO_2 and 37 °C. After 48 h of incubation, cells overexpressing *pcDNA-CaV1.2* or the vector only were washed with Hanks balanced buffer (HBH) containing (mmol/l): NaCl (137), KCl (5.4), $MgSO_4$*$7H_2O$ (0.4), KH_2PO_4(0.4), $CaCl_2$*$2H_2O$ (1.3), Na_2HPO_4*$7H_2O$ (0.3), and HEPES (20, pH 7.4), and 0.1% BSA twice and then lysed with a hand homogenizer on ice for 2 min in lysis buffer containing HEPES (20 mmol/l) and 0.1% NP40. Thereafter, the cell lysates (50 μg protein per lane) were used for Western blot analysis [4] to verify overproduction of CaV1.2 in the transfected cells.

For pull-down assays, lysates (500 μg protein per sample) of cells transfected with the vector or *pcDNA-CaV1.2* were incubated with or without REG2 protein (2 μg) in Tris buffer (25 mmol/l, pH 7.2) overnight at 4 °C on a rotation wheel. The binding complex was incubated with REG2 antibody (1 μg, R&D Systems, MAB2098) or rat IgG (Thermo Fisher, 31933, Supplemental Table 2) for 8 h and then with protein G beads (Santa Cruz, Dallas, TX) for 1 h at 4 °C on rotation wheel. The beads were collected by centrifugation, and incubated with the loading buffer of Western blot at 95 °C for 5 min to release the pulled-down CaV1.2 protein complex. The released protein was immunoblotted using CaV1.2 antibody (Alomone labs, ACC-003) [4].

To determine if REG2 could still pull down deglycosylated Cav1.2, we expressed *pcDNA-CaV1.2* or the vector in Min6 cells as described above in beta TC3 cells for 3 d. The transfected cells were lysed in 0.25% trypsin-EDTA, separated by ultracentrifuge (100,000 g, 90 min) to collect membrane fraction, and re-suspended in a deglycosylation buffer (pH 7.8) containing 1%NP-40, 150 mmol NaCl/l, 50 mmol Tris-HCl/l, and protease inhibitor cocktail (Thermo Scientific, 784251). The lysate suspension (1 mg protein) was incubated with or without a deglycosylase (PNGase F, 20 μl, 10,000 units, New England Biolabs, P0704S) for 7 h at 37 °C. Subsequently, the mixture was incubated with REG2 protein (4 μg) for 6 h before with REG2 antibody (4 μg) or rat IgG isotype (Supplemental Table 2) for 12 h at 4 °C on a rotation wheel. The immune-precipitated complex was collected by adding 40 μl of protein G-PLUS agarose (4 °C on a rotation wheel for 2 h, Santa Cruz Biotechnology, sc02003) and spinning down the beads. The target CaV1.2 in the precipitate was tested as described above.

2.5. Ligand and receptor binding of REG2 and CaV1.2 in betaTC-3 cells

To test if REG2 could bind CaV1.2 overexpressed on the membrane of beta TC-3 cells, we generated *alkaline phosphatase* (*AP*)*-Reg2/Reg2 M1* constructs by inserting the *Reg2* and *Reg2 M1* DNA fragments into an AP tag-5 vector (GenHunter, Nashville, TN) (Supplemental Tables 1 and 3). After transfection of the plasmids (5 μg DNA) into HEK293T cells (seeded at 2.2 × 10^6/plate, 90% confluency at transfection, ATCC, Manassas, Virginia) with polyethylenimine (PEI) [33], cells were incubated in DMEM (Gibco) containing 10% FBS and 1% PenStrep at 37 °C, 5% CO_2 for 4 d before collecting the condition media (CM) containing secreted AP-REG proteins. The AP activity in the CM was measured using *para*-nitrophenylphosphate (PNPP, Sigma-Aldrich) as the substrate [34].

After beta TC-3 cells (seeded in 24-well plates at 5 × 10^4/well, 80% confluency at transfection) were transfected with the *pcDNA-CaV1.2* plasmid for 48 h as described above, cells were washed with HBH containing HEPES (20 mmol/l, pH 7.4), and 0.1% BSA twice, and incubated with 0.5 ml of CM (AP, AP-REG2, or AP-REG2 M1) with or without CaV1.2 antibody (1 μg/ml) or REG2 protein (1 μg/ml) for 2 h at room temperature [33]. Cells were further washed with ice cold HBH for 3 times and then fixed with 3.7% formaldehyde for 20 min on plates. After fixing, cells were washed with HBH buffer again and the plates were put in 67 °C incubator for 5 h [35]. After the endogenous AP activity was deactivated, cells were washed with AP buffer containing Tris-HCl (100 mmol/l, pH 9.5), 100 mmol NaCl/l, and 5 mmol $MgCl_2$/l and incubated with nitro blue tetrazolium chloride (NBT) [70 μL; stock 50 mg/ml in 70% dimethylformamide (DMF)] and 5-bromo-4-chloro-3-indolyl phosphate (BCIP, 70 μl; stock 25 mg/ml in H_2O) in 10 ml AP buffer [36] to develop the color (AP activity). Ligand-receptor binding was shown by the AP activity on cell surface (the color increase) [37] and the change in shading/dark pixels were measured using software ImageJ.

2.6. Co-localization of REG2 and CaV1.2 in beta TC-3 cells

To test co-localization of REG2 with CaV1.2 in beta TC-3 cells, we modified the *AP-Reg2 and Reg2 M1* vectors by replacing *AP* with *EGFP* to form *Gfp/Gfp–Reg2/Reg2 M1* constructs (Addgene, Supplemental Tables 1 and 3). The plasmids were transfected into HEK293T cells to

produce CM as described above (for the AP-REG2 binding assay). Expression of GFP-REG2 protein was measured using an Axiovert 200 M fluorescent microscope (Zeiss, Carl-Zeiss-Strasse, Oberkochen, Germany). Meanwhile, the *CaV1.2* gene was inserted into *pmCherry-C3* vector (Addgene, Supplemental Table 3) to generate *pmCherry-CaV1.2-C3* plasmid and transfected into betaTC-3 cells as described above. The co-localization assay was run with six different combinations of two sources of CaV1.2 (cells transfected with *pmCherry* and *pmCherry-CaV1.2*) and three types of CM proteins (GFP, GFP-REG2, and GFP-REG2 M1). After 48 h of transfection, cells (seeded in μ-Dish, 35 mm high, Ibidi, Germany, at 3×10^5/dish, 90% confluence at transfection) were washed twice with HBH buffer and incubated with CM containing GFP, GFP-REG2, or GFP-REG2 M1 proteins for 2 h at room temperature. Thereafter, cells were washed 3 times with ice cold HBH and viewed using a Confocal-MP Inverted microscope (Zeiss 880, Carl-Zeiss-Strasse, Oberkochen, Germany). The relative percentage of yellow fluorescence area (% of GFP positive cells in mCherry positive cells) was scored using MetaMorph® image analysis software (Molecular Devices) and was used as the indicator of co-localization.

2.7. Effects of REG2 on Ca^{2+} influx in cultured and perifused islets

To determine if the binding of REG2 to CaV1.2 affected Ca^{2+} influx, we performed Ca imaging of cultured OE islets and perifused WT islets loaded with fluo 4-acetoxymethyl ester (Fluo 4-AM, Thermo Fisher Scientific, Waltham, MA, F1242) [38] and Fura 2-AM (Molecular Probes, Eugene, OR) [39], respectively. In the static culture, isolated OE islets were recovered for 12 h in RPMI 1640 media (10% FBS, 2 mmol glutamine/l, 10 mmol glucose/l, and 1% PenStrep), washed with Krebs buffer (with 2.8 mmol glucose/l), and incubated with 2 μmol Fluo 4-AM/l for 2 h at 37 °C and 5% CO2. Thereafter, the islets were washed with Krebs buffer (2.8 mmol glucose/l) for 4 times and incubated with either PBS or REG2 (1 μg/ml) in Krebs buffer (2.8 mmol glucose/l) for 15 min before respective stimulations of glucose (2.8, 16.7, and 30 mmol/l) and KCl (30 mmol/l). Fluorescence was imaged using an Axiovert 200 M Fluorescent Microscope (Zeiss, Filter set 09; set the peak excitation at 490 nm and the peak emission at 516 nm) before and after (5 min) the stimulations.

In the perifusion system, isolated WT islets were recovered in RPMI 1640 media as described above for 12 h at 37 °C and 5% CO_2. After a 40-min pretreatment at 37 °C in 2 ml of Krebs buffer supplemented with Fura 2-AM (1 μmol/l), the loaded islet was transferred to a perifusion chamber and placed on the homeothermic platform of an inverted Zeiss AxioVision microscope. Islets were perfused with Krebs buffer at 37 °C at a flow rate of 2 ml/min, while REG2 (1 μg/ml, PBS as the control) was added into the perifusate continuously or for a given period of time. In the former (continuous) case (n = 4), the islet was perifused with 3 mmol glucose/l for 10 min and then REG2 (1 μg/ml) was added in the perifusate with glucose at 3 mmol/l for 15 min, at 16.7 mmol/l for 15 min, and at 3 mmol/l for 7 min and with KCl at 30 mmol/l for 8 min. In the latter (on/off) case (n = 9), the islet was perifused with glucose at 3 mmol/l for 15 min and at 16.7 mmol glucose/l for 10 min. Subsequently, REG2 (1 μg/ml) was added into the perifusate in which glucose concentration was maintained at 16.7 mmol/l for 10 min. Thereafter. REG2 was removed from the perifusate and the perifusion was continued to run with glucose at 16.7 mmol/l for 10 min and at 3 mmol/l for 10 min and with KCl at 30 mmol/l for 8 min. Intracellular Ca^{2+} concentrations were determined by ratios of fluorescence (Fura 2-AM) detected at excitation wavelength of 340 (Ca^{2+} complex) to 380 (free anion) nm with the emission wavelength at 520 nm using an Attofluor charge-coupled device camera, and calibrated by the Attofluor Ratio Vision Software [31].

2.8. Statistical analysis

Genotype differences in islet gene expression and protein production (n = 6) and various treatment effects of REG2 verse PBS/buffer controls (n = 4 to 10) were analyzed using Student *t*-test and one-way ANOVA (SAS 6.11 software, SAS Institute, Cary, NC). Values were expressed as mean ± SEM. Significance was defined as $p < 0.05$.

3. Results

3.1. REG2 was depleted by GPX1 overproduction in OE islets

Compared with WT mice, OE mice had moderate elevations (32–50%, $p < 0.05$) of *Ins1, Pdx1,* and *Foxa2* mRNA levels in pancreatic islets (Fig. 1A). There were no significant genotype differences in islet mRNA levels of *Reg1* or other 14 insulin-related genes (Supplemental Fig. 1). In contrast, *Reg2* mRNA in OE islets was decreased to only 0.7–7% ($p < 0.05$) of that in WT islets across the three tested ages of mice (Fig. 1B). OE islets showed a similar decrease ($p < 0.05$) in transcript numbers of *Reg2,* but not *Reg1* compared with WT islets (Fig. 1C). Likewise, REG2 protein in OE islets was decreased ($p < 0.05$) to < 10% of that in WT islets (Fig. 1D). These results depicted a consistent diminishing of REG2 gene expression and(or) protein production in OE islets.

3.2. Inhibition of GSIS by REG2 required its C-type lectin domain

The verified REG2 depletion in OE islets led us to test if augmented GSIS in these islets could be inhibited or rescued by treating them with exogenous REG2. Compared with PBS-treated controls, the REG2 (1 μg/mL) treatment (for 0.5 h) did not affect insulin secretion of OE islets cultured at 2.8 mmol glucose/l, but the treatment (for 1 h) decreased insulin secretion (30%, $p < 0.05$) of OE islets cultured at 30 mmol glucose/l (Fig. 2A). In perifused OE islets, the REG2 treatment (1 μg/ml) suppressed the overall GSIS by 41% ($p < 0.05$) compared with the buffer-treated control (Fig. 2C). The inhibition became significant when the glucose ramp reached approximately 15 mmol glucose/l and was maintained up to 50 mmol glucose/l. The REG2 perifusion also caused substantial decreases ($p < 0.05$) in insulin secretion stimulated by KCl (30 mmol/l). In contrast, REG2 M1 (with mutations in the C-lectin binding domain) showed a major loss of the inhibition on GSIS (Fig. 2D). Meanwhile, REG2 M2 (with mutations in the acid residue domain) retained a moderate inhibition on the high side of glucose ramp (Fig. 2E). Although both mutants decreased KCl-induced insulin secretions, their effects were not statistically significant. Apparently, REG2 exerted a potent inhibition on GSIS in OE islets, and the C-type lectin domain was required for the inhibition because mutating the domain in REG2 M1 abolished the inhibition. In comparison, the retained moderated inhibition by REG2 M2 on GSIS implied that the acidic residues could modulate (decrease) the inhibition, but were not essential for the action. The loss of a significant inhibition on the KCl-stimulated insulin secretion by the two mutants in comparison with REG2 implied the importance of both C-type lectin domain and acidic residues in the regulation.

3.3. Co-immunoprecipitation of REG2 and CaV1.2 required glycosylation of CaV1.2

The inhibition by REG2, but not REG2 M1 on GSIS and the recognized role of CaV1.2 in regulating glucose-stimulated elevation of Ca^{2+} influx and insulin secretion [25] gave us a strong rationale to determine if REG2, through its C-type lectin binding domain, bound the carbohydrate moiety of CaV1.2 to exert the inhibition. After lysates of beta TC3 cells overproducing CaV1.2 (Fig. 3A) were incubated with REG2 protein, REG2 antibody was able to pull down CaV1.2 from the mixture (Fig. 3B). This pull down was seen only from the mixture added with both REG2 protein and antibody, indicating a specific co-immunoprecipitation of CaV1.2 via binding to REG2. In contrast, the same REG2 antibody failed to pull down CaV1.2 from the mixture when

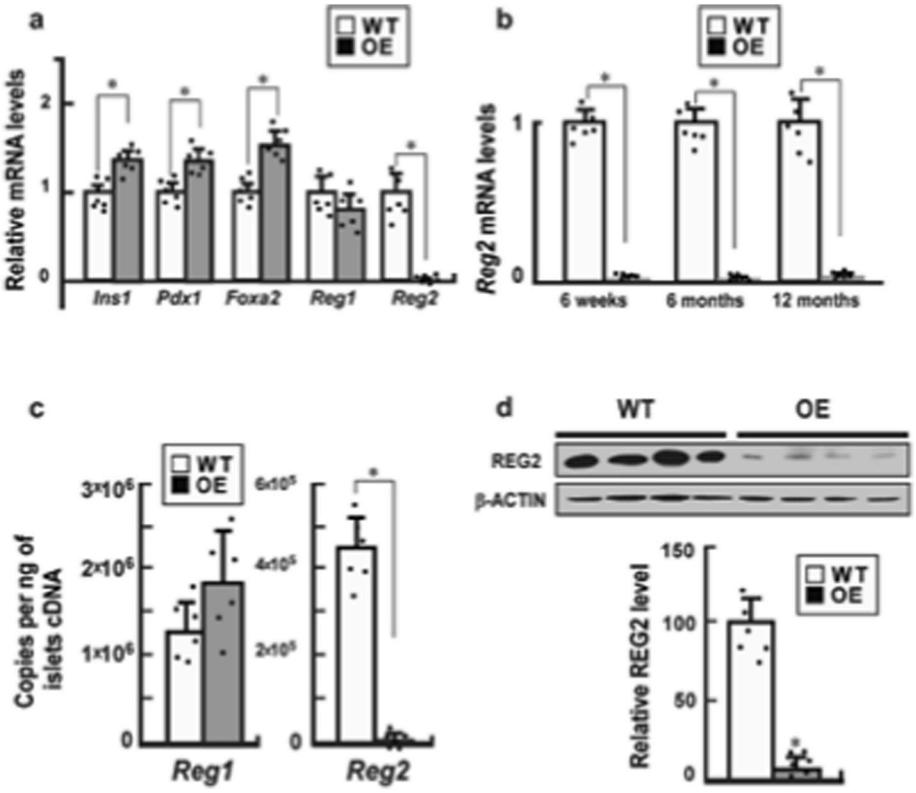

Fig. 1. Depletion of REG2 mRNA, transcript, and protein in pancreatic islets of mice by GPX1 overproduction

Relative mRNA levels of *Ins1*, *Pdx1*, *Foxa2*, *Reg1*, and *Reg2* in pancreatic islets (70 per sample) of OE mice to those of WT (as 1) mice (2-month old, male, n = 6) after normalization with the respective beta-actin mRNA (A), depletion of *Reg2* mRNA in pancreatic islets (70 per sample) of OE mice across three ages compared with the WT (as 1) mice (male, n = 6) after normalization with the respective beta-actin mRNA levels (B), comparisons of *Reg1* and *Reg2* transcript numbers/ng cDNA in pancreatic islets (70 per sample) between OE and WT mice (6-month old, male, n = 6) (C), depletion of REG2 protein in pancreatic islets (75 μg protein per sample) of OE mice compared with WT mice (6-month old, male, n = 4) shown by immunoblotting (upper panel, a representative of four independent experiments), and relative densities (lower panel) of bands were quantified with Image J (the WT as 100) after normalization with beta-actin protein density. Data are mean ± SE, *, $p < 0.05$ for differences between genotypes.

lysates of Min6 cells overproducing CaV1.2 were deglycosylated (Fig. 3C). The CaV1.2 α1c subunit was detected in the immuno-precipitates with only glycosylated but not deglycosylated CaV1.2 in the cell lysates, verifying the essential role of the carbohydrate moiety of CaV1.2 in this putative binding.

3.4. Binding of REG2 to CaV1.2 required the C-type lectin binding domain of REG2

Because only REG2 M1 (with mutations in the C-type lectin domain), but not REG2 M2 (with mutations in the acidic residues), lost most of the inhibition on GSIS, we focused subsequent CaV1.2 binding assays with REG2 and REG2 M1. Incubating beta TC3 cells overexpressing CaV1.2 with AP-REG2 produced a 1.4-fold increase ($p < 0.05$) in the color staining (shading/dark pixels), compared with that in cells transfected with the vector only (Fig. 3D). The increased intensity was resulted from the enhanced AP reactions with NBT and BCIP, indicating an elevated ligand-receptor binding between AP-REG2 and CaV1.2 on the cell surface. However, neither AP-REG2 M1-treated nor AP-treated cells showed such an increase. Furthermore, that increase produced by the AP-REG2 treatment was attenuated (30–45%) by incubations of CaV1.2 antibody or excessive REG2 protein (unconjugated with AP) via competitive binding to CaV1.2. In the control cells transfected with the vector only, the AP-REG2 treatment also produced ~ 3-fold AP activity (staining, $p < 0.05$) of that treated by AP-5, suggesting a binding of AP-REG2 to the endogenous CaV1.2. These results revealed that the over-expressed or endogenous, transmembrane CaV1.2 in beta TC3 cells indeed bound extracellular REG2. The binding was displayed as a specific, competitive ligand-receptor interaction, and required the presence of C-type lectin binding domain in REG2.

3.5. Only REG2, but not REG2 M1, was co-localized with CaV1.2

After the pull down and AP-tag binding assays, we performed a co-immunofluorescence analysis to generate another evidence for the putative binding between REG2 and CaV1.2. Incubating CaV1.2-mCherry-overexpressing beta TC3 cells with GFP-REG2 yielded yellow fluorescence (Fig. 3E). The overlap of the green (GFP-REG2) and the red (CaV1.2-mCherry) fluorescence was verified from 4 different views (Supplemental Fig. 4). The relative percentage of yellow fluorescence area was nearly tripled ($p < 0.05$) by the GFP-REG2 incubation over the control. In contrast, little change in the fluorescence (yellow) was produced by either REG2 (without being conjugated with GFP) or GFP-REG2 M1 (mutations in the C-type lectin binding domain). Once again, only GFP-REG2, but not GFP-REG2 M1, when added extracellularly, was found to bind or co-localize with CaV1.2 overexpressed in beta TC3 cells.

3.6. Binding of REG2 to CaV1.2 decreased glucose-stimulated Ca^{2+}influx in islets

To explore metabolic impacts of the above-tested binding of REG2 to CaV1.2, we determined if that binding affected Ca^{2+} influx of OE and WT islets stimulated by glucose or KCl. Compared with PBS, REG2 substantially attenuated or blocked the fluorescence enhancements of Fluo 4-AM (increases in Ca^{2+} influx) caused by glucose (16.7 and 30 mmol/l) and KCl (30 mmol/l) (Fig. 4A). The fluorescence increases in the PBS-treated OE islets after these stimulations were in an ascending order of 16.7 and 30 mmol glucose/l and 30 mmol KCl/l, with little change in those islets continuously incubated with 2.8 mmmol glucose/l. In addition, only REG2 and nifedipine (a CaV1.2 inhibitor), but not REG2 M1 or PBS, decreased the 30 mM glucose-induced increase of Ca^{2+} influx in the cultured OE islets (Supplemental Fig. 5).

When REG2 was added continuously into the perifusate starting at 3 mmol glucose/l, the inhibition of REG2 on Ca^{2+} influx appeared only when the glucose concentration in the ramp reached 16.7 mmol/l (Fig. 4B). The overall inhibition was 25% ($p < 0.05$, REG2 vs. buffer control). Meanwhile, adding REG2 in the perifusate for 10 min after the glucose concentration reached 16.7 mmol/l quickly suppressed the Ca^{2+} influx by 17% ($p < 0.05$ vs. without REG2) (Fig. 4C). The inhibition

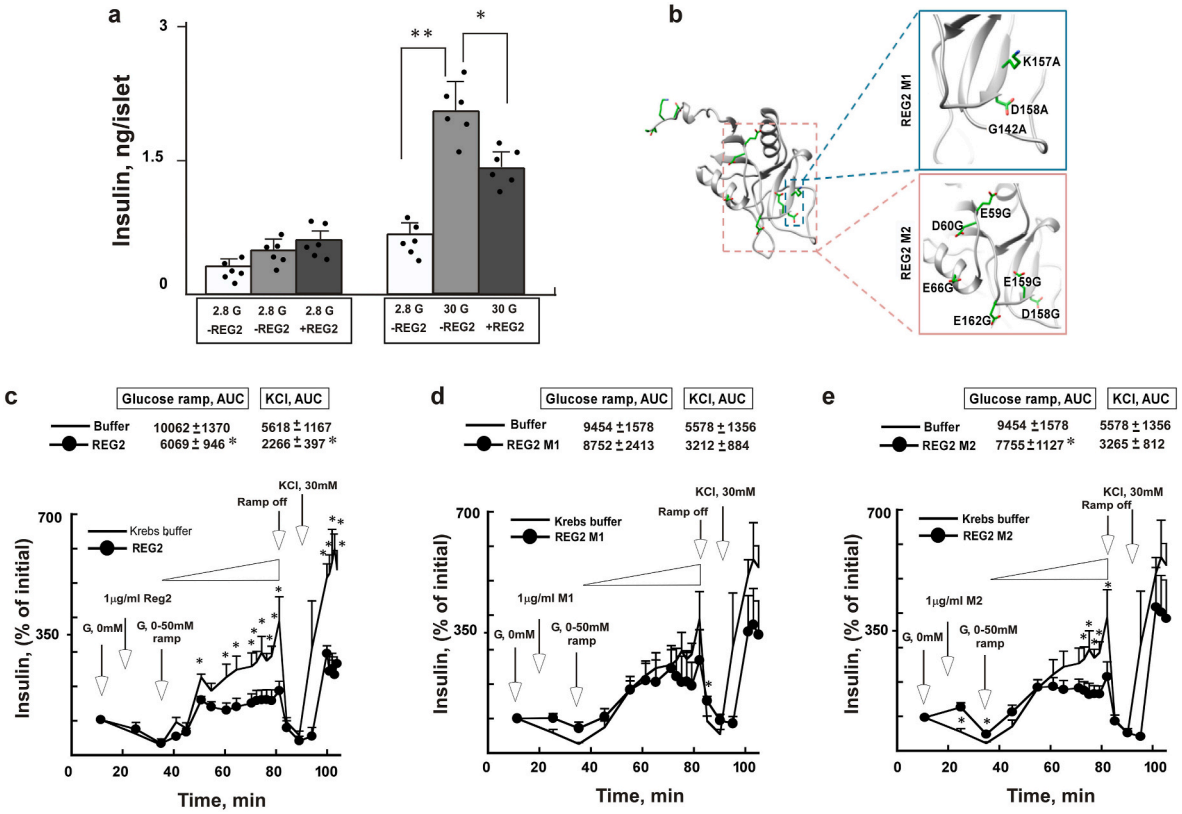

Fig. 2. Inhibition of glucose-stimulated insulin secretion by exogenous REG2.
Effects of REG2 (1 μg/mL) on insulin secretion of in static cultured islets (70 per sample) of OE mice (2-month old, male, n = 4) at 2.8 mmol glucose (2.8 G) for 0.5 h or 30 mmol glucose/l (30 G) for 1 h (A), an illustration of designed mutations in the C-type lectin binding domain (REG2 M1) and the acidic residues (REG2 M2) based on predicted three-dimensional protein structure of REG2 (B), effects of REG2 (C), REG2 M1 (D) and REG2 M2 (E) (1 μg/mL) on GSIS of perifused (1 ml/min) islets (70 per sample) of OE mice (2-months old, male, n = 4 per treatment) in comparison with those of Krebs buffer. In all panels (except for B), data are mean ± SE, *, $p < 0.05$ for differences between REG2 or REG2 M2 verse buffer or PBS controls. In panel A, **, $p < 0.05$ for difference between 2.8 G and 30 G in insulin secretion. In panels C, D, and E, values on the top are areas under curve (AUC) of insulin secretion stimulated by glucose or KCl for the perifusion with buffer or REG2 and mutants, *$p < 0.05$ for difference between the buffer and treatments (REG2 or REG2 M2); G: glucose; mM, mmol/l; and the gradient bar above the trace: glucose ramp from 0 to 50 mmol/l.

disappeared or the Ca^{2+} influx was restored ($p < 0.05$ vs. with REG2) after REG2 was removed from the perifusate (Fig. 4C). In both settings, REG2 was able to inhibit the Ca^{2+} influx induced by 16.7 and(or) 30 mmol glucose/l and 30 mmol KCl/l in OE and WT islets. The inhibition was acute and reversible, with minimal effects at the baseline or low glucose concentrations (2.8 or 3 mmol/l).

3.7. *Exogenous REG2 administration inhibited GSIS in OE mice*

To explore the physiological relevance and clinical potential of the inhibition on GSIS by REG2 in islets, we gave OE mice an ip injection of the purified recombinant REG2 protein. Compared with PBS, the REG2 injection (2 μg/g of body weight) to OE mice decreased their overall plasma insulin concentration by 46% ($p < 0.05$, Fig. 5A) and elevated their overall plasma glucose concentration by 25% ($p < 0.05$, Fig. 5B) during a 60 min period after glucose challenge. This depicted an *in vivo* effectiveness of the exogenous REG2 administration.

4. Discussion

The present study reveals a novel role and mechanism of REG2 depletion in the augmented GSIS of OE islets [2]. Specifically, REG2 transcript and protein in OE islets were depleted by GPX1 overproduction. Administrations of exogenous REG2 inhibited GSIS in OE islets and mice, and the inhibition required the C-type lectin binding domain in the protein. Exogenous or extracellular REG2 could pull down, bind, and co-localize with VDCC protein CaV1.2 overexpressed in beta TC3 cells, indicating a ligand-receptor binding between REG2 and CaV1.2. This putative binding required the C-type lectin binding domain of REG2 and glycosylation of CaV1.2, and suppressed glucose- and KCl-stimulated Ca^{2+} influx in cultured OE islets and perifused WT islets. Along with our previous findings [2–4], the present study identifies a novel GPX1/REG2/CaV1.2 cascade to help explain how the REG2 depletion in OE islets could decrease its binding to CaV1.2, resulting in uninhibited Ca^{2+} influx and insulin secretion after glucose stimulation. Because GPX1 overproduction initiates or drives this cascade [4] and dietary Se deficiency [3], but not diet restriction [2], precludes GPX1 overproduction in OE mice, it is now conceivable that only the former but not the latter prevented the augmented GSIS in those mice [2,3]. Linking GPX1 overproduction to GSIS and Ca^{2+} influx through regulating REG2 production and its interactions with CaV1.2 provides a new paradigm to describe long-term metabolic mechanisms for GPX1 and other redox enzymes [40] as modulator of intracellular ROS [41]. While physiological levels of intracellular peroxides are required to trigger GSIS [42,43], there are various impacts of transient or acute elevation of intracellular ROS on oxidative modifications of protein kinases or phosphatases related to insulin signaling [43–45], excessive ROS on expression and function of beta cell-related transcriptional factors [46–48], and chronic exposure of ROS on blunting signaling of GSIS [49,50]. Clearly, our findings add a new mode of action or pathway for redox enzymes and ROS to regulate GSIS and perhaps other metabolic events.

The inhibition of GSIS by REG2 was demonstrated in both OE islets

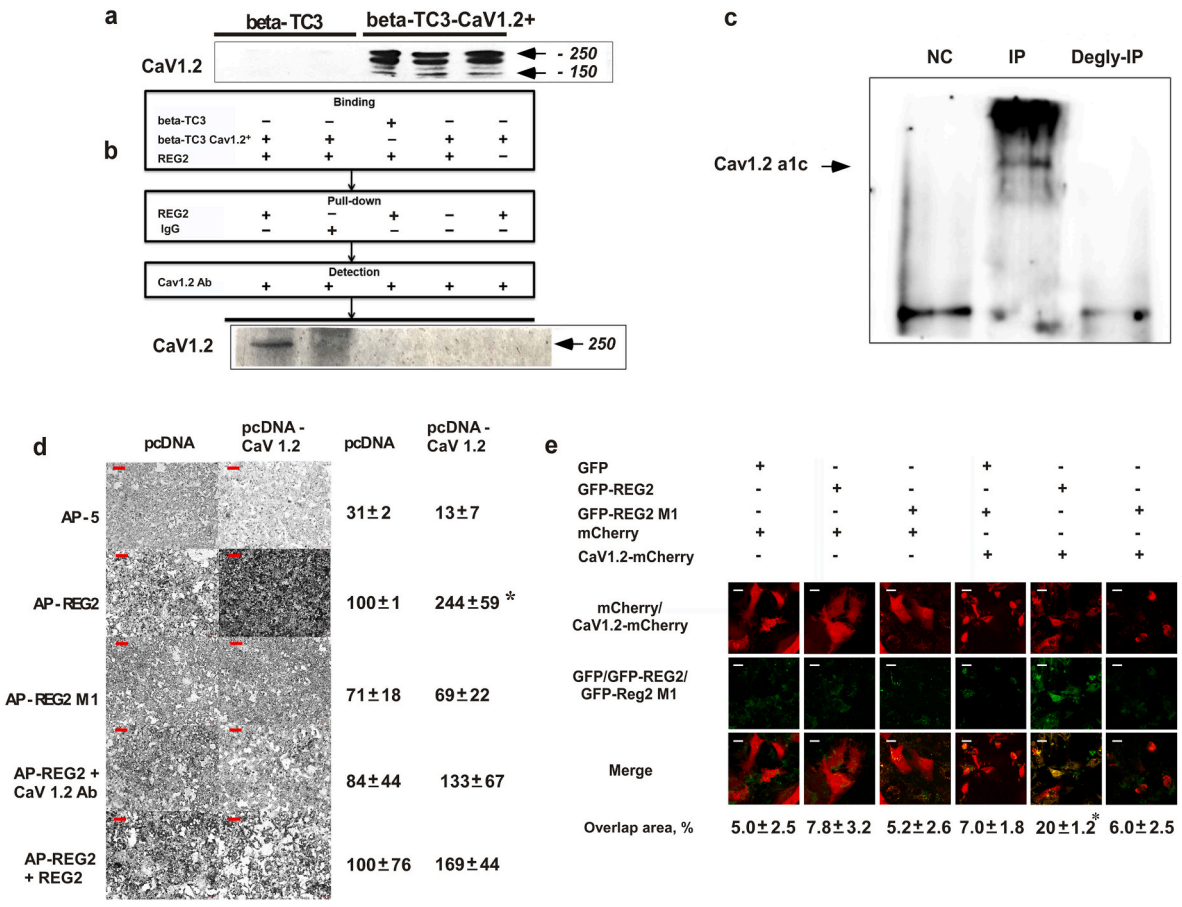

Fig. 3. Evidences for a ligand-receptor binding between REG2 and CaV1.2.
Western blot analysis of CaV1.2 protein produced by beta TC3 cells (50 μg protein per lane) transfected with *pcDNA* vector and *pcDNA-CaV1.2* plasmid (A), co-immunoprecipitation of CaV1.2 protein with REG2: the lysates (500 μg protein per sample) of beta-TC3 cells transfected with *pcDNA-CaV1.2* plasmid were incubated with REG2 protein (2 μg) and REG2 antibody (1 μg) and the precipitates were collected by protein G beads and immunoblotted against CaV1.2 antibody (B), co-immunoprecipitation of REG2 with glycosylated verse deglycosylated CaV1.2 in lysates of Min6 cells transfected with *pcDNA-CaV1.2* plasmid: cell lysates (1 mg protein per sample) were treated with or without PNGase F (20 μl, 10,000 units) and incubated with REG2 protein (2 μg) and REG2 antibody (1 μg); the precipitates were collected by protein G beads and immunoblotted against CaV1.2 antibody; and the CaV1.2 α1c subunit was detected only in the precipitated cell lysates without deglycosylation (C), the putative ligand-receptor binding of alkaline phosphatase (AP)-conjugated REG2 (AP-REG2) vs. AP-REG2 M1 and AP (1 μg/ml) overexpressed and secreted by HEK293T cells to CaV1.2 on the surface of beta TC3 cells transfected with *pcDNA* vector or *pcDNA-CaV1.2* plasmid in the presence or absence of CaV1.2 antibody (1 μg/ml) or REG2 (1 μg/ml), and the extent of binding was shown by the retained AP activity on cell surface and quantitated (the right box) by the shading/dark pixels using software Image J (D), co-immunofluorescence of green fluorescence protein (GFP)-conjugated REG2 (GFP-REG2) vs. GFP-REG2 and GFP (1 μg/ml) overexpressed and secreted by HEK293T cells with mCherry-CaV1.2 on the surface of beta TC3 cells transfected with *pmCherry* vector or *pcmCherry-CaV1.2* plasmid for 48 h, and the relative percentage of yellow fluorescence area (% of GFP positive cells in mCherry positive cells) was scored using MetaMorph image analysis software (E). In panels A, B, and C, the images were representative of 4 independent experiments. In panels of D and E, scale bar = 10 μm; values are mean ± SE from four independent experiments; $p < 0.05$ for differences between REG2 and respective controls. (For interpretation of the references to color in this figure legend, the reader is referred to the Web version of this article.)

and mice. When the mutations of the C-type lectin binding domain in REG2 M1 led to a loss of inhibition on GSIS and Ca^{2+} influx, the variant was no longer able to bind to or co-localize with CaV1.2 in beta TC3 cells. Clearly, the C-type lectin binding domain in REG2 was essential for the inhibition. In contrast, mutating the acidic residues of REG2 (REG2 M2) retained a moderate inhibition of GSIS on the high side of glucose ramp. The acidic residues in hREG1α were shown to be involved in $CaCO_3$ binding [8] and were highly conserved between the mouse REG2 and hREG1α (Supplemental Fig. 3). Seemingly, these residues might be involved in, but not essential, for the inhibition. Neither mutant (REG2 M1 or M2) exhibited significant inhibition on the KCl-induced insulin release. We do not have a clear structure explanation to this. Although we used relatively high glucose concentrations (30 or 50 mM) to stimulate the islets, our glucose ramp covered a wide range of GSIS from minimal to above maximal physiological concentrations. The perifused REG2 maintained similar inhibitions on GSIS from 15 mmol glucose/l to the end of glucose ramp, indicating a broad effectiveness of REG2 at both physiological and superphysiological glucose conditions. Such a broad spectrum of REG2 action was shown by its effects on GSIS and glucose tolerance in the OE mice that were hyperglycemia and hyperinsulinemia [1]. Consistently, REG2 exerted comparable inhibitions on Ca^{2+} influx induced by 16.7 and 30 mmol glucose/l and 30 mmol KCl/l in OE islets, and reversible inhibition on the 16.7 mmol glucose-induced Ca^{2+} influx in the WT islets. Notably, REG2 displayed little or insignificant effect on insulin secretion or Ca^{2+} influx induced by low glucose concentrations including 2.8 and 3 mM in OE and(or) WT islets.

Demonstrating effectiveness of exogenous REG2 in inhibiting GSIS of OE islets and mice has biomedical implications. Firstly, it confers a new role for REG2 other than beta cell proliferation [5] and regeneration [19, 51]. Although trophic functions have been an exclusive focus of REG2 research since its discovery [6], a lack of impact by the *Reg2* deletion in young mice [12] on beta cell proliferation failed to support that premise. Secondly, illustrating the inhibition on GSIS by exogenous REG2 in OE islets and mice provides a direct evidence for the proposed endo-, para-

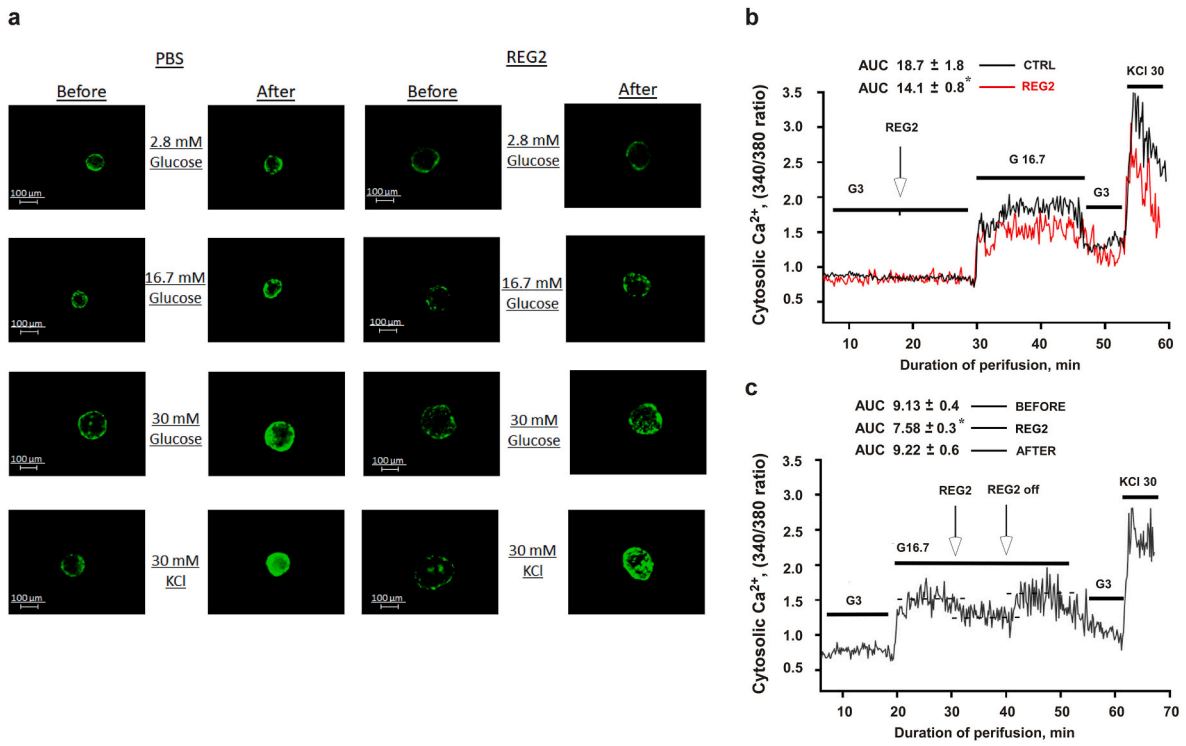

Fig. 4. Inhibition of Ca^{2+} influx in pancreatic islets of OE and WT mice by exogenous REG2

Effects of REG2 (1 μg/ml) vs. PBS on Ca^{2+} influx, measured by fluorescence of Fluo 4-AM (2 μmol/l, with the peak excitation wavelength at 490 nm and the peak emission wavelength at 516 nm), in islets (50 per sample) of OE mice (6-month old, male) before and after (5 min) stimulations of glucose (2.8, 16.7, and 30 mmol/l) and KCl (30 mmol/l) (A), effects of a continuous perifusion of REG2 (1 μg/ml, labeled in red verse buffer, labeled in black) on the Ca^{2+} influx, measured by fluorescence ratio of Fura 2-AM (2 μmol/l) at excitation wavelengths of 340 (Ca-bound) to 380 (free anion) with emission wavelength of 520, in single islets (n = 4) of WT mice (6-month old, male) perifused with glucose (3 and 16.7 mmol/l) and KCl (30 mmol/l) (B), rapid and reversible inhibition of the Ca^{2+} influx by REG2 (1 μg/mL), measured as in B, in single-perifused islets (n = 9) of WT mice (the same as in B) after the glucose ramp reached 16.7 mmol/l and the loss of inhibition after the removal of REG2 from the perifusate (C). In panel A, fluorescence was imaged using an Axiovert 200 M Fluorescent Microscope (Zeiss, Filter set 09). In panels B and C, an inverted Zeiss AxioVision microscope with Attofluor ration vision software was used to record the time course of intracellular Ca concentration changes. The overall inhibition (B) by REG2 vs buffer and the reversible inhibition of REG2 vs before and after the removal of REG2 at the same glucose concentration (16.7 mmol/l) (C) were expressed as AUC (area under curve), *p < 0.05 vs control. (For interpretation of the references to color in this figure legend, the reader is referred to the Web version of this article.)

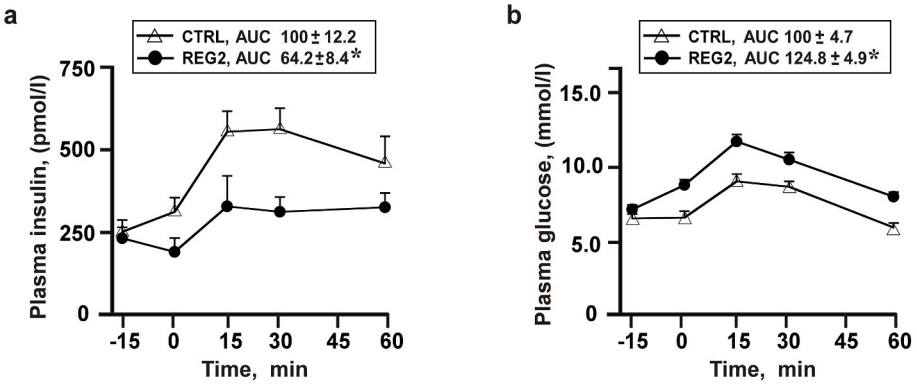

Fig. 5. In vivo effects of exogenous REG2 administration to OE mice.

Effects of an intraperitoneal (ip) injection of REG2 (2 μg/g body weight), in comparison with an equal volume (10 μL/g body weight) of phosphate-buffed saline (PBS), to male OE mice (6 months old, n = 10) at 15 min before a glucose challenge (ip, 1 g/kg body weight) on plasma concentrations of insulin (A) and glucose (B) over 60 min. Data are mean ± SE, *, $p < 0.05$ for area under curve (AUC) of REG2 verse PBS.

and autocrine functions of the protein [9]. It may underscore metabolic potentials for REG2 secreted by cultured islets into media [4] and by exocrine pancreas under various stress conditions [9,10,12]. Intriguingly, the old *Reg2−/−* mice showed an impaired GSIS [12], whereas our REG2-depleted OE mice displayed an augmented GSIS [2]. This GSIS-phenotype discrepancy may be partially explained by the decreased beta cell proliferation and mass in the former in contrast to the hypertrophy of beta cells, upregulation of pancreatic and duodenal homeobox 1 (PDX1) and insulin synthesis, and down-regulation of uncoupling protein 2 in the latter. Nevertheless, it will be interesting to find out if repeated injections of REG2 to both OE and WT mice for an extended time affect their pancreatic beta cell mass and insulin synthesis, in addition to GSIS. Conversely, it will be relevant to determine if glucose exposure and uptake affect REG2 expression and function in islets.

It is exciting to reveal the ligand-receptor binding of REG2 to CaV1.2 in beta TC3 cells and the subsequent effect on the glucose-stimulated Ca^{2+} influx in OE and WT islets. This finding represents a dual

breakthrough in the field, which qualifies REG2 as a novel regulator of CaV1.2 and CaV1.2 as a new cognate receptor/binding protein of REG2. None of the REG proteins has been shown to bind CaV1.2 or affect its role in Ca^{2+} influx and GSIS [25–28,52]. Although the REG family proteins are a group of secretory proteins requiring transmembrane receptors to exert their functions, only exostosin like glycosyltransferase 3 (EXTL3) and epidermal growth factor receptor (EGFR) were shown as the receptor of or to bind human REG1α and human and mouse REG3A [37,53,54]. Despite the presence of the C-type lectin binding domain in all REG proteins, only the present study has succeeded in finding CaV1.2 as one of those transmembrane proteins with a carbohydrate moiety to bind that domain of REG2.

Clarifications, cautions, and future research may be required to interpret our novel findings. Notably, the physiological sources and routes of REG2 for regulating GSIS need a precise characterization. This is because production or secretion of REG2 by endocrine cells of pancreas remains uncertain [9,10,12]. Result discrepancies among different groups may arise from genetic background or (and) age-dependent and pancreatic-specific expressions of mouse REG2 [10] and specificity of reagents (antibodies) [4,13–15]. The same controversy also exists on expression of the putative human orthologue hREG1β in beta cells [55] or islets [18]. However, the highly expressed hREG1β, as a relatively small molecule found in the blood, in exocrine pancreas [16] might reach islets to affect GSIS. Meanwhile, the effectiveness of exogenous REG2 administration in inhibiting GSIS in OE mice may suggest a distant pre-clinical potential of using hREG1β and its antagonists to treat GSIS disorders in hyperinsulinemic and diabetic patients. While GPX1 is considered to protect against various chronic diseases [56–58], *GPX1* polymorphism [59–63] and (or) GPX activity alterations [64–69] are associated with insulin-related disorders. However, the exact pathological implication of the GPX1/REG2/CaV1.2 cascade in T2DM and other diseases remains a future research question, because changes of REG2 in different types of T2DM were not unilateral [4,20].

The revealed ligand-receptor interaction between REG2 and CaV1.2 may be substantiated by performing Ca^{2+} current measurements in depolarized beta cells in the absence and presence of REG2 and the mutants. Because CaV1.2 and other VDCC proteins contain not only the α1c but also α2δ1 subunit [23,24], it will be useful to test if REG2 binds the α1c subunit directly or via an auxiliary subunit, and if the inhibition on GSIS is mainly due to this liagnd-receptor binding or partially related to functions of peptides of REG2 degradation [14]. It will also be important to find out how the mutations of acidic residues in REG2 retained some inhibition on GSIS, but lost most inhibition on the KCl-stimulated insulin release, if the inhibition on GSIS by REG2 involves both Ca^{2+}-influx-triggered and metabolically amplified steps, and how differences between human and mouse β-cells in the expression of other Ca^{2+-}channels [70] affects the REG2 interaction with the L-type channels.

5. Conclusion

Our laboratory previously demonstrated that overproduction of GPX1 led to augmented GSIS and depletion of REG2 via transcriptional inhibition in pancreatic islets of mice. Because REG2 contains a canonical C-type lectin binding domain that could potentially interact with glycoproteins on cell surface to regulate GSIS, we have explored the role and mechanism of REG2 in binding L-voltage-dependent Ca^{2+} channel CaV1.2, a transmembrane protein with key roles in the glucose-stimulated elevation of Ca^{2+} influx and the induced insulin exocytosis. Our results have revealed a potent inhibition by REG2 on GSIS and(or) the glucose-induced Ca^{2+} influx in cultured and perifused islets and(or) mice, along with a ligand-receptor binding of REG2 to CaV1.2 and their co-localization in beta cells. Altogether, our work identifies a novel pathway of GPX1/REG2/CaV1.2 in regulating GSIS and creates new links to bridge redox biology, tissue regeneration, and insulin secretion.

Data and resource availability

Data sharing: Datasets generated and/or analyzed during the current study are available from corresponding authors upon reasonable request.

Resource sharing

Resources generated during the current study are available from corresponding authors upon reasonable request.

Funding

This research was supported by a NIH grant DK53018 (to XGL).

Declaration of competing interest

Xi Yan, Zeping Zhao, Jeremy Weaver, Tao Sun, Jun-Won Yun, Fenghua Hu, Nicolai M. Doliba, Marko Z. Vatamaniuk, and Xin Gen Lei, no conflict of interest.

Contributions of authors

X.Y. and Z.P.Z contributed equally to designing and performing experiments, analyzing data, and writing the manuscript. J.-W.Y. helped in determining *Reg2* expression. J. W. helped in designing, producing, and testing the native and mutant REG2 proteins. CAR helped the immuneblotting. T.S. performed the co-immunoprecipitation of deglycosylated CaV1.2 and the Ca^{2+} influx in the cultured islets. N.M.D. helped the Ca^{2+} influx assay in the perifused islets. F. H. helped in performing the AP-Tag and mCherry assays. CCM and HS helped the data interpretation and the manuscript writing. M.Z.V. contributed to experimental design, bioinformatics of REG2, islets perfusion experiments, data analysis, and manuscript preparation. X.G.L conceived, designed, and supervised this research and was responsible for writing the final version of the manuscript. XY and CAR take responsibilities of data presented in Figs. 1 and 2; XY, ZZ, TS, and NMD take responsibilities of data presented in Figs. 3–5. XGL and MZV are the guarantor of this work and, as such, have full access to all the data in the study and takes responsibility for the integrity of the data and the accuracy of the data analysis.

Data availability

Data will be made available on request.

Acknowledgments

We would like to thank Professor Helmut Sies for his insightful review and editing of the manuscript.

The NOD mouse *Reg2* cDNA (NM_009043, G22 to A173) was kindly provided by Dr. Werner Gurr (Yale University, New Haven, CT). The REG2 antibody was a generous gift from Dr. M. Bishr Omary (Stanford University Digestive Disease Center, Stanford, CA). The beta TC3 and Min6 cells were kindly provided by Dr. Qiaoming Long (Cornell University, Ithaca, NY). Krystal Lum (Cornell University, Ithaca, NY) assisted the cloning and expression of REG2 proteins. M.Z.V and N.M.D. dedicate their contribution of the paper to Professor Vyacheslav Korobov, a former advisor, a teacher, and a friend who was an inspirational scientist and an outstanding person.

Appendix A. Supplementary data

Supplementary data to this article can be found online at https://doi.org/10.1016/j.redox.2022.102457.

References

[1] J.P. McClung, C.A. Roneker, W. Mu, et al., Development of insulin resistance and obesity in mice overexpressing cellular glutathione peroxidase, Proc. Natl. Acad. Sci. USA 101 (24) (2004) 8852–8857.

[2] X. Wang, M. Vatamaniuk, S. Wang, C. Roneker, R. Simmons, X. Lei, Molecular mechanisms for hyperinsulinaemia induced by overproduction of selenium-dependent glutathione peroxidase-1 in mice, Diabetologia 51 (8) (2008) 1515–1524.

[3] X. Yan, M.P. Pepper, M.Z. Vatamaniuk, C.A. Roneker, L. Li, X.G. Lei, Dietary selenium deficiency partially rescues type 2 diabetes–like phenotypes of glutathione peroxidase-1–overexpressing male mice, J. Nutr. 142 (11) (2012) 1975–1982.

[4] J.-W. Yun, Z. Zhao, X. Yan, M.Z. Vatamaniuk, X.G. Lei, Glutathione peroxidase-1 inhibits transcription of regenerating islet-derived protein-2 in pancreatic islets, Free Radic. Biol. Med. 134 (2019) 385–393.

[5] J.-L. Liu, W. Cui, B. Li, Y. Lu, Possible roles of reg family proteins in pancreatic islet cell growth. Endocrine, Metabolic & Immune Disorders-Drug Targets, (Formerly Current Drug Targets-Immune, Endocrine & Metabolic Disorders) 8 (1) (2008) 1–10.

[6] M. Unno, H. Yonekura, K-i Nakagawara, et al., Structure, chromosomal localization, and expression of mouse reg genes, reg I and reg II. A novel type of reg gene, reg II, exists in the mouse genome, J. Biol. Chem. 268 (21) (1993) 15974–15982.

[7] J.R. Walker, B. Nagar, N.M. Young, T. Hirama, J.M. Rini, X-ray crystal structure of a galactose-specific C-type lectin possessing a novel decameric quaternary structure, Biochemistry 43 (13) (2004) 3783–3792.

[8] J.A. Bertrand, D. Pignol, J.-P. Bernard, J.-M. Verdier, J.-C. Dagorn, J.C. Fontecilla-Camps, Crystal structure of human lithostathine, the pancreatic inhibitor of stone formation, EMBO J. 15 (11) (1996) 2678–2684.

[9] B. Zhong, P. Strnad, D.M. Toivola, et al., Reg-II is an exocrine pancreas injury-response product that is up-regulated by keratin absence or mutation, Mol. Biol. Cell 18 (12) (2007) 4969–4978.

[10] Y. Wang, C. Jacovetti, B. Li, et al., Coordinated age-dependent and pancreatic-specific expression of mouse Reg2 Reg3α, and Reg3β genes, Growth Factors 29 (2–3) (2011) 72–81.

[11] R. Perfetti, J.M. Egan, M.E. Zenilman, A.R. Shuldiner, Differential expression of reg-I and reg-II genes during aging in the normal mouse, J. Gerontol. Ser. A: Biol. Sci. Med. Sci. 51 (5) (1996) B308–B315.

[12] Q. Li, B. Li, X. Miao, C. Ramgattie, Z-h Gao, J.-L. Liu, Reg2 expression is required for pancreatic islet compensation in response to aging and high-fat diet–induced obesity, Endocrinology 158 (6) (2017) 1634–1644.

[13] M.M. Rankin, J.A. Kushner, Aging induces a distinct gene expression program in mouse islets, Islets 2 (6) (2010) 345–352.

[14] W. Gurr, M. Shaw, Y. Li, R. Sherwin, RegII is a β-cell protein and autoantigen in diabetes of NOD mice, Diabetes 56 (1) (2007) 34–40.

[15] W. Gurr, The role of Reg proteins, a family of secreted C-type lectins, in islet regeneration and as autoantigens in type 1 diabetes, Type 1 (2011) 161–182.

[16] D. Sanchez, C. Figarella, S. Marchand-Pinatel, N. Bruneau, O. Guy-Crotte, Preferential expression of reg Iβ gene in human adult pancreas, Biochem. Biophys. Res. Commun. 284 (3) (2001) 729–737.

[17] M. Uhlén, L. Fagerberg, B.M. Hallström, et al., Proteomics. Tissue-based map of the human proteome, Science (New York, N.Y.) 347 (6220) (2015), 1260419, 1260419.

[18] Å. Segerstolpe, A. Palasantza, P. Eliasson, et al., Single-cell transcriptome profiling of human pancreatic islets in health and type 2 diabetes, Cell Metabol. 24 (4) (2016) 593–607.

[19] D.D. De León, C. Farzad, M.F. Crutchlow, et al., Identification of transcriptional targets during pancreatic growth after partial pancreatectomy and exendin-4 treatment, Physiol. Genom. 24 (2) (2006) 133–143.

[20] L. Qiu, E.O. List, J.J. Kopchick, Differentially expressed proteins in the pancreas of diet-induced diabetic mice, Mol. Cell. Proteomics 4 (9) (2005) 1311–1318.

[21] J. Lazniewska, N. Weiss, Glycosylation of voltage-gated calcium channels in health and disease, Biochim. Biophys. Acta Biomembr. 1859 (5) (2017) 662–668.

[22] V. Mastrolia, S.M. Flucher, G.J. Obermair, et al., Loss of α2δ-1 calcium channel subunit function increases the susceptibility for diabetes, Diabetes 66 (4) (2017) 897–907.

[23] D.J. Triggle, 1, 4-Dihydropyridines as calcium channel ligands and privileged structures, Cell. Mol. Neurobiol. 23 (3) (2003) 293–303.

[24] H. Glossmann, D.R. Ferry, F. Lübbecke, R. Mewes, F. Hofmann, Identification of voltage operated calcium channels by binding studies: differentiation of subclasses of calcium antagonist drugs with 3H-nimodipine radioligand binding, J. Recept. Res. 3 (1–2) (1983) 177–190.

[25] S.-N. Yang, P.-O. Berggren, The role of voltage-gated calcium channels in pancreatic β-cell physiology and pathophysiology, Endocr. Rev. 27 (6) (2006) 621–676.

[26] V. Schulla, E. Renström, R. Feil, et al., Impaired insulin secretion and glucose tolerance in β cell-selective Cav1. 2 Ca2+ channel null mice, EMBO J. 22 (15) (2003) 3844–3854.

[27] M.D. Nitert, C.L. Nagorny, A. Wendt, L. Eliasson, H. Mulder, CaV1. 2 rather than CaV1. 3 is coupled to glucose-stimulated insulin secretion in INS-1 832/13 cells, J. Mol. Endocrinol. 41 (1) (2008) 1–12.

[28] P. Buda, T. Reinbothe, V. Nagaraj, et al., Eukaryotic translation initiation factor 3 subunit e controls intracellular calcium homeostasis by regulation of cav1. 2 surface expression, PLoS One 8 (5) (2013), e64462.

[29] J.D. Weaver, A.H. Ullah, K. Sethumadhavan, E.J. Mullaney, X.G. Lei, Impact of assay conditions on activity estimate and kinetics comparison of Aspergillus Niger PhyA and Escherichia coli AppA2 phytases, J. Agric. Food Chem. 57 (12) (2009) 5315–5320.

[30] D. Zhao, Y.-H. Kim, S. Jeong, et al., Survival signal REG3α prevents crypt apoptosis to control acute gastrointestinal graft-versus-host disease, J. Clin. Invest. 128 (11) (2018) 4970–4979.

[31] M.Z. Vatamaniuk, R.K. Gupta, K.A. Lantz, N.M. Doliba, F.M. Matschinsky, K. H. Kaestner, Foxa1-deficient mice exhibit impaired insulin secretion due to uncoupled oxidative phosphorylation, Diabetes 55 (10) (2006) 2730–2736.

[32] G.L. Pittenger, D.A. Taylor-Fishwick, R.H. Johns, N. Burcus, S. Kosuri, A.I. Vinik, Intramuscular injection of islet neogenesis-associated protein peptide stimulates pancreatic islet neogenesis in healthy dogs, Pancreas 34 (1) (2007) 103–111.

[33] M. Yamabhai, B.K. Kay, Mapping protein-protein interactions with alkaline phosphatase fusion proteins, in: Methods in Enzymology, vol. 332, Elsevier, 2001, pp. 88–102.

[34] E. Van Koetsveld, The determination of the alkaline serum phosphatase activity with barium-p-nitrophenylphosphate as a substrate, Acta Physiol. Pharmacol. Neerl. 2 (2) (1951) 276–279.

[35] J.G. Flanagan, P. Leder, The kit ligand: a cell surface molecule altered in steel mutant fibroblasts, Cell 63 (1) (1990) 185–194.

[36] J.J. Leary, D.J. Brigati, D.C. Ward, Rapid and sensitive colorimetric method for visualizing biotin-labeled DNA probes hybridized to DNA or RNA immobilized on nitrocellulose: bio-blots, Proc. Natl. Acad. Sci. USA 80 (13) (1983) 4045–4049.

[37] Y. Wu, Y. Quan, Y. Liu, et al., Hyperglycaemia inhibits REG3A expression to exacerbate TLR3-mediated skin inflammation in diabetes, Nat. Commun. 7 (1) (2016) 1–14.

[38] K.L. Corbin, H.L. West, S. Brodsky, N.B. Whitticar, W.J. Koch, C.S. Nunemaker, A practical guide to rodent islet isolation and assessment revisited, Biol. Proced. Online 23 (1) (2021) 1–21.

[39] K.L. Corbin, T.E. Hall, R. Haile, C.S. Nunemaker, A novel fluorescence imaging approach for comparative measurements of pancreatic islet function in vitro, Islets 3 (1) (2011) 14–20.

[40] R. Brigelius-Flohé, E.S.J. Arnér, Selenium and selenoproteins in (redox) signaling, diseases, and animal models - 200 year anniversary issue, Free Radic. Biol. Med. 127 (2018) 1–2, https://doi.org/10.1016/j.freeradbiomed.2018.09.026.

[41] H. Sies, Hydrogen peroxide as a central redox signaling molecule in physiological oxidative stress: oxidative eustress, Redox Biol. 11 (2017) 613–619.

[42] C. Leloup, C. Tourrel-Cuzin, C. Magnan, et al., Mitochondrial reactive oxygen species are obligatory signals for glucose-induced insulin secretion, Diabetes 58 (3) (2009) 673–681.

[43] B.J. Goldstein, K. Mahadev, X. Wu, Redox paradox: insulin action is facilitated by insulin-stimulated reactive oxygen species with multiple potential signaling targets, Diabetes 54 (2) (2005) 311–321.

[44] K. Loh, H. Deng, A. Fukushima, et al., Reactive oxygen species enhance insulin sensitivity, Cell Metabol. 10 (4) (2009) 260–272.

[45] M. Ishiki, Y. Nishida, H. Ishibashi, et al., Impact of divergent effects of astaxanthin on insulin signaling in L6 cells, Endocrinology 154 (8) (2013) 2600–2612.

[46] R.P. Robertson, J.S. Harmon, Diabetes, glucose toxicity, and oxidative stress: a case of double jeopardy for the pancreatic islet β cell, Free Radic. Biol. Med. 41 (2) (2006) 177–184.

[47] J. Pi, Y. Bai, Q. Zhang, et al., Reactive oxygen species as a signal in glucose-stimulated insulin secretion, Diabetes 56 (7) (2007) 1783–1791.

[48] X. Wang, M.Z. Vatamaniuk, C.A. Roneker, et al., Knockouts of SOD1 and GPX1 exert different impacts on murine islet function and pancreatic integrity, Antioxidants Redox Signal. 14 (3) (2011) 391–401.

[49] R.P. Robertson, Chronic oxidative stress as a central mechanism for glucose toxicity in pancreatic islet beta cells in diabetes, J. Biol. Chem. 279 (41) (2004) 42351–42354.

[50] X. Wang, J.-W. Yun, X.G. Lei, Glutathione peroxidase mimic ebselen improves glucose-stimulated insulin secretion in murine islets, Antioxidants Redox Signal. 20 (2) (2014) 191–203.

[51] K. Huszarik, B. Wright, C. Keller, et al., Adjuvant immunotherapy increases β cell regenerative factor Reg2 in the pancreas of diabetic mice, J. Immunol. 185 (9) (2010) 5120–5129.

[52] A. Davalli, E. Biancardi, A. Pollo, et al., Dihydropyridine-sensitive and-insensitive voltage-operated calcium channels participate in the control of glucose-induced insulin release from human pancreatic β cells, J. Endocrinol. 150 (2) (1996) 195–203.

[53] I.A.-T. Van Ba, S. Marchal, F. François, et al., Regenerating islet-derived 1α (Reg-1α) protein is new neuronal secreted factor that stimulates neurite outgrowth via exostosin Tumor-like 3 (EXTL3) receptor, J. Biol. Chem. 287 (7) (2012) 4726–4739.

[54] X. Liu, J. Wang, H. Wang, et al., REG3A accelerates pancreatic cancer cell growth under IL-6-associated inflammatory condition: involvement of a REG3A–JAK2/STAT3 positive feedback loop, Cancer Lett. 362 (1) (2015) 45–60.

[55] R. Planas, A. Alba, J. Carrillo, et al., Reg (regenerating) gene overexpression in islets from non-obese diabetic mice with accelerated diabetes: role of IFNβ, Diabetologia 49 (10) (2006) 2379–2387.

[56] J.B. de Haan, P.J. Crack, N. Flentjar, R.C. Iannello, P.J. Hertzog, I. Kola, An imbalance in antioxidant defense affects cellular function: the pathophysiological consequences of a reduction in antioxidant defense in the glutathione peroxidase-1 (Gpx1) knockout mouse, Redox Rep. 8 (2) (2003) 69–79, https://doi.org/10.1179/135100003125001378.

[57] D.E. Handy, J. Loscalzo, The role of glutathione peroxidase-1 in health and disease, Free Radic. Biol. Med. 188 (2022) 146–161, https://doi.org/10.1016/j.freeradbiomed.2022.06.004.
[58] L.A. Seale, D.J. Torres, M.J. Berry, M.W. Pitts, A role for selenium-dependent GPX1 in SARS-CoV-2 virulence, Am. J. Clin. Nutr. 112 (2) (2020) 447–448, https://doi.org/10.1093/ajcn/nqaa177.
[59] P. Vats, N. Sagar, T. Singh, M. Banerjee, Association of superoxide dismutases (SOD1 and SOD2) and glutathione peroxidase 1 (GPx1) gene polymorphisms with type 2 diabetes mellitus, Free Radic. Res. 49 (1) (2015) 17–24.
[60] M. Banerjee, P. Vats, Reactive metabolites and antioxidant gene polymorphisms in type 2 diabetes mellitus, Redox Biol. 2 (2014) 170–177.
[61] C.Á. Hernández Guerrero, P. Hernández Chávez, N. Martínez Castro, A. Parra Carriedo, S. García del Río, A.B. Pérez Lizaur, Glutathione Peroxidase-1 Pro200Leu Polymorphism (rs1050450) Is Associated with Morbid Obesity Independently of the Presence of Prediabetes or Diabetes in Women from Central Mexico, 2015.
[62] M. Kuzuya, F. Ando, A. Iguchi, H. Shimokata, Glutathione peroxidase 1 Pro198Leu variant contributes to the metabolic syndrome in men in a large Japanese cohort, Am. J. Clin. Nutr. 87 (6) (2008) 1939–1944.
[63] T. Ramprasath, P.S. Murugan, E. Kalaiarasan, P. Gomathi, A. Rathinavel, G. S. Selvam, Genetic association of Glutathione peroxidase-1 (GPx-1) and NAD (P) H: quinone Oxidoreductase 1 (NQO1) variants and their association of CAD in patients with type-2 diabetes, Mol. Cell. Biochem. 361 (1) (2012) 143–150.
[64] X. Chen, T.O. Scholl, M.J. Leskiw, M.R. Donaldson, T.P. Stein, Association of glutathione peroxidase activity with insulin resistance and dietary fat intake during normal pregnancy, J. Clin. Endocrinol. Metab. 88 (12) (2003) 5963–5968.
[65] J. Bleys, A. Navas-Acien, S. Stranges, A. Menke, E.R. Miller III, E. Guallar, Serum selenium and serum lipids in US adults, Am. J. Clin. Nutr. 88 (2) (2008) 416–423.
[66] M.-S. Zeng, X. Li, Y. Liu, et al., A high-selenium diet induces insulin resistance in gestating rats and their offspring, Free Radic. Biol. Med. 52 (8) (2012) 1335–1342.
[67] J. Zhou, K. Huang, X.G. Lei, Selenium and diabetes—evidence from animal studies, Free Radic. Biol. Med. 65 (2013) 1548–1556.
[68] V.M. Labunskyy, B.C. Lee, D.E. Handy, J. Loscalzo, D.L. Hatfield, V.N. Gladyshev, Both maximal expression of selenoproteins and selenoprotein deficiency can promote development of type 2 diabetes-like phenotype in mice, Antioxidants Redox Signal. 14 (12) (2011) 2327–2336.
[69] A. Pinto, B. Speckmann, M. Heisler, H. Sies, H. Steinbrenner, Delaying of insulin signal transduction in skeletal muscle cells by selenium compounds, J. Inorg. Biochem. 105 (6) (2011) 812–820.
[70] M. Braun, R. Ramracheya, M. Bengtsson, et al., Voltage-Gated ion channels in human pancreatic β-cells: electrophysiological characterization and role in insulin secretion, Diabetes 57 (6) (2008) 1618–1628, https://doi.org/10.2337/db07-0991.